Title
Allosteric Inhibition of a Vesicular Glutamate Transporter by an Isoform-Specific Antibody

Journal
Biochemistry, 60(32)

ISSN
0006-2960

Authors
Eriksen, Jacob
Li, Fei
Stroud, Robert M
et al.

Publication Date
2021-08-17

DOI
10.1021/acs.biochem.1c00375

Peer reviewed

Published in final edited form as:

Biochemistry. 2021 August 17; 60(32): 2463–2470. doi:10.1021/acs.biochem.1c00375.

Allosteric Inhibition of a Vesicular Glutamate Transporter by an Isoform-Specific Antibody

Jacob Eriksen,
Departments of Neurology and Physiology, UCSF School of Medicine, San Francisco, California 94143, United States

Fei Li,
Departments of Neurology and Physiology and Department of Biochemistry and Biophysics, UCSF School of Medicine, San Francisco, California 94143, United States

Robert M. Stroud,
Department of Biochemistry and Biophysics, UCSF School of Medicine, San Francisco, California 94143, United States

Robert H. Edwards
Departments of Neurology and Physiology, UCSF School of Medicine, San Francisco, California 94143, United States

Abstract

The role of glutamate in excitatory neurotransmission depends on its transport into synaptic vesicles by the vesicular glutamate transporters (VGLUTs). The three VGLUT isoforms exhibit a complementary distribution in the nervous system, and the knockout of each produces severe, pleiotropic neurological effects. However, the available pharmacology lacks sensitivity and specificity, limiting the analysis of both transport mechanism and physiological role. To develop new molecular probes for the VGLUTs, we raised six mouse monoclonal antibodies to VGLUT2. All six bind to a structured region of VGLUT2, five to the luminal face, and one to the cytosolic. Two are specific to VGLUT2, whereas the other four bind to both VGLUT1 and 2; none detect VGLUT3. Antibody 8E11 recognizes an epitope spanning the three extracellular loops in the C-domain that explains the recognition of both VGLUT1 and 2 but not VGLUT3. 8E11 also inhibits both glutamate transport and the VGLUT-associated chloride conductance. Since the antibody

Corresponding Author Robert H. Edwards – Phone: (415) 502-5687; robert.edwards@ucsf.edu.

Author Contributions

J.E. performed immunostainings and the VGLUT functional experiment. F.L. prepared VGLUT for immunization, did the biochemical characterization of antibodies, and determined the structure. All authors designed and analyzed experiments. J.E. and R.H.E. wrote the paper with input from F.L. and R.M.S.

ASSOCIATED CONTENT

Supporting Information

The Supporting Information is available free of charge at https://pubs.acs.org/doi/10.1021/acs.biochem.1c00375.

Western Blot probing VGLUT2-EGFP with VGLUT2 mAbs and EGFP antibody; mAbs 8E11 and 9C6 heavy and light chain amino acid sequences; sequence alignment of ECL4-6 from VGLUT1-3 (PDF)

Accession Codes

VGLUT1 (rat): Uniprot entry Q62634. VGLUT2 (rat): Uniprot entry Q9JI12. VGLUT3 (rat): Uniprot entry Q7TSF2.

The authors declare no competing financial interest.

Complete contact information is available at: https://pubs.acs.org/10.1021/acs.biochem.1c00375

binds outside the substrate recognition site, it acts allosterically to inhibit function, presumably by restricting conformational changes. The isoform specificity also shows that allosteric inhibition provides a mechanism to distinguish between closely related transporters.

Graphical Abstract

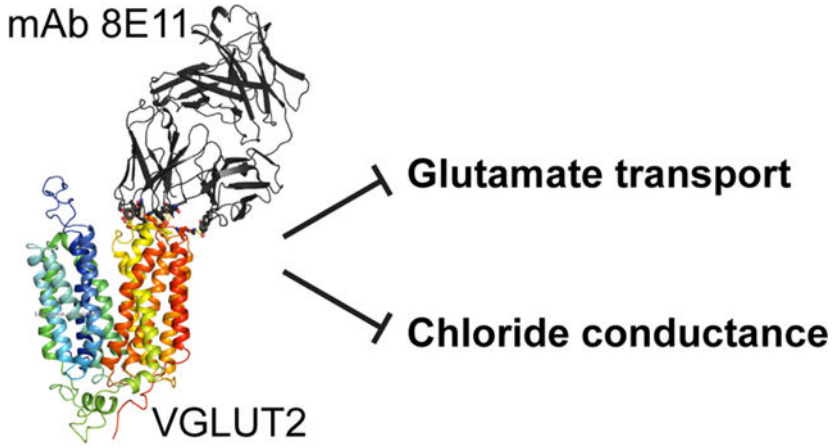

The exocytic release of glutamate mediates most excitatory transmission in the mammalian nervous system. Packaging into synaptic vesicles enables glutamate release by exocytosis and involves uptake from the cytoplasm by the vesicular glutamate transporters (VGLUTs). A proton electro-chemical gradient across the synaptic vesicle membrane generated by the vacuolar-type H^+-ATPase provides the driving force for vesicular glutamate transport, similar to the other vesicular neurotransmitter transporters.[1,2] In contrast to other vesicular neurotransmitter transporters driven by proton exchange, glutamate uptake relies on membrane potential as the main driving force,[3,4] suggesting a mechanism of facilitated diffusion. However, additional ions including protons and chloride regulate vesicular glutamate transport, acting allosterically to coordinate flux with other events in the synaptic vesicle cycle.[5]

Mammals express three VGLUT isoforms, VGLUT1 (SLC17A7), VGLUT2 (SLC17A6), and VGLUT3 (SLC17A8). The three transporters exhibit high sequence identity, especially in the transmembrane domains that make up the translocation pathway. They also do not seem to differ in intrinsic transport activity. However, they differ greatly in distribution, conferring distinct physiological roles.[6,7] VGLUT1 is expressed primarily in the cortex, VGLUT2 in the diencephalon and brainstem,[8,9] and VGLUT3 often by neurons associated with a different transmitter.[10–12]

Consistent with their different distributions, genetic inactivation of each VGLUT isoform produces profound but distinct neurological effects.[7,12–15] However, acute inactivation has not been possible due to the lack of specific inhibitors. The relatively low apparent affinity for glutamate (K_m = 1–3 mM) has presumably contributed to the difficulty of identifying high-affinity VGLUT inhibitors. Indeed, glutamate analogues such as aminocyclopentane-1,2-dicarboxylate and methylated forms of glutamate inhibit the VGLUTs with high micromolar potency, only slightly higher affinity than glutamate

itself.[16,17] Through unclear mechanisms, several azo dyes including Evans Blue, Chicago Sky Blue, and Brilliant Yellow inhibit much more potently,[18,19] in the low nanomolar range but lack specificity for the VGLUTs[20] and cell permeability.[21] All of these compounds act as competitive inhibitors, and high homology within the binding pockets presumably accounts for the lack of specificity for the VGLUT isoform. More recently, two nanobodies were raised against VGLUT1, and these recognize the cytoplasmic face of the transporter.[22] They also inhibit glutamate transport, but the isoform specificity and mechanism of inhibition are not known. Here we describe the production of several antibodies to VGLUT2 that distinguish among the isoforms and show that one inhibits transport through an allosteric mechanism.

MATERIALS AND METHODS

Antibodies.

Monoclonal antibodies (mAb) against N- and C-terminally truncated rat VGLUT2 were produced as previously described[23] with VGLUT2 proteoliposomes as antigen injected into mice at the Vaccine and Gene Therapy Institute (VGTI) Monoclonal Antibody Core of Oregon Health Sciences University. The antibody variable domains of hybridomas 8E11 and 9C6 were sequenced by Genscript.

Immunofluorescence.

Fixed Cells.—HEK293T cells at 90–95% confluency in 6-well plates were transfected with 2 μg pIRES2-EGFP encoding a plasma membrane-targeted version of rat VGLUT (pmVGLUT) 1, 2, or 3 (Uniprot entries: Q62634, Q9JI12, and Q7TSF2) with 6 μL of FugeneHD according to the manufacturer's protocol. The next day, the cells were seeded onto 12 mm glass coverslips coated with poly-L-lysine (1 mg/mL) in 24 well plates. One day later, the cells were washed in PBS and fixed in PBS containing 4% PFA for 30 min on ice. After fixation, the cells were washed 3 times in PBS before blocking and permeabilization in PBS with 5% goat serum and 0.1% Triton X-100 for 30 min. The cells were incubated with hybridoma supernatants diluted 1:20 in blocking buffer for 1 h at room temperature, washed 3 times for 10 min each in PBS, incubated with goat antimouse antibody conjugated to Alexa Fluor 647 (1:500) in blocking buffer for 30 min at room temperature, washed three times in PBS for 10 min each, and the coverslips mounted using VECTASHIELD Antifade Mounting Medium.

Live Antibody Feeding.—Live HEK293T cells were incubated with hybridoma supernatants diluted 1:20 in full growth media for 30 min at rt, washed three times for 5 min each in PBS before fixation and blocking as above. The samples were then incubated with goat antimouse antibody conjugated to Alexa Fluor 647, washed, and mounted as above.

Imaging and Quantification.—The specimens were imaged using a Nikon Ti inverted microscope equipped with a CSU-22 spinning disk confocal and a Plan Apo VC 60×/1.4 oil objective. Imaging settings were identical for all samples, and all images were processed using ImageJ. To quantify the mAb fluorescence, an ROI was created over transfected cells

using the EGFP signal as a template. The total Alexa Fluor 647 signal was measured for each of the ROIs.

Glutamate Efflux.

HEK293T cells were transfected with pIRES2-EGFP pmVGLUT2 or pIRES2-EGFP as a control using Fugene HD as described above. The next day, the cells were moved into 24-well plates coated with poly-L-lysine (0.1 mg/mL). Another day later, the cells were rinsed twice in Ringer's solution (145 mM NaCl, 10 mM glucose, 10 mM HEPES pH 7.4, 4 mM KCl, 2 mM $CaCl_2$, 1 mM $MgCl_2$) before loading with 25 μM ^{3}H-glutamate (2 μCi) in 200 μL of Ringer's solution without or with 8E11 (1:100) for 15 min at 37 °C. The cells were then washed three times in ice-cold Ringer's solution containing 0.5 mM aspartate. Glutamate efflux was measured in 200 μL of warm Ringer's solution or Ringer's solution at pH 5.5 (145 mM NaCl, 10 mM glucose, 10 mM MES pH 5.5, 4 mM KCl, 2 mM $CaCl_2$, 1 mM $MgCl_2$) with 0.5 mM aspartate for 5 min at 37 °C. A total of 150 μL of the medium was collected and the radioactivity measured by scintillation counting. The efflux was analyzed by normalizing the efflux cpm to pH 7.4 + 8E11.

Oocyte Recordings.

Recordings were performed as described previously.[24] Briefly, *Xenopus laevis* oocytes were obtained from Ecocyte, injected with 50 ng of pmVGLUT2-HA cRNA, and incubated in ND96 (96 mM NaCl, 2 mM KCl, 1.8 mM $CaCl_2$, 1 mM $MgCl_2$, 5 mM HEPES [pH 7.4]) with 50 μg/mL tetracycline and gentamicin at 16 °C for 5 days. The oocyte currents were recorded by a standard two-electrode voltage clamp in Ca^{2+}−free ND96 and ND96 pH 5.5 (96 mM NaCl, 2 mM KCl, 1 mM $MgCl_2$, 5 mM MES [pH 5.5]). Steady-state current/voltage (I–V) relations were obtained using a protocol of 300 ms voltage steps from −120 to +60 in 10 mV steps from a holding potential of −30 mV. After first running the step protocol at pH 7.4 and pH 5.5 without antibody, 2 μL of 8E11 or control EAT-4 antibody 8A9 was added to the recording chamber, the oocytes were incubated for 10 min, and excess antibody was removed by perfusion in ND96 pH 7.4 before recording at pH 7.4 and pH 5.5.

RESULTS

To generate probes capable of recognizing a structured domain of the VGLUTs, we injected mice with purified rat VGLUT2 reconstituted into liposomes.[23] The immunized mice yielded multiple monoclonal antibody hybridomas. Using supernatant from the hybridomas, we tested their binding to HEK293T cells expressing an internalization-defective, plasma membrane-targeted version of VGLUT2 (pmVGLUT2).[24] All six of the tested antibodies show binding to fixed, permeabilized cells expressing pmVGLUT2 (identified by the coexpressed EGFP), whereas nontransfected ($EGFP^-$) cells in the confluent cultures show no binding (Figure 1A,C).

The use of pmVGLUT2 enabled us to determine whether the antibodies bind to either the luminal or cytoplasmic face of the transporter. Live cells expressing pmVGLUT2 can only be stained by antibodies that recognize the luminal/external face of VGLUT2, whereas antibodies recognizing the cytoplasmic face will not have access to this site in

cells with an intact plasma membrane (Figure 1B). Supernatants from hybridomas 6D3, 8E11, 9C6, 12C1, and 14E1 all give rise to a high fluorescent signal in HEK293T cells expressing pmVGLUT2 (Figure 1B,C), showing that these antibodies bind to the luminal surface of VGLUT2. In contrast, 13H4, which shows specific binding to VGLUT2 in fixed, permeabilized cells, does not show any signal above the background with intact cells. Thus, 13H4 binds to the cytoplasmic face of VGLUT2, similar to the nanobodies recently reported.[22]

We then assessed the isoform specificity of the antibodies by immunostaining cells expressing plasma membrane-targeted versions of VGLUT1 or VGLUT3. Supernatants from hybridomas 6D3, 8E11, 9C6, and 12C1 all bind to pmVGLUT1-expressing cells, whereas 13H4 and 14E1 show no binding (Figure 2A,C). None of the antibodies show any binding to cells expressing pmVGLUT3 (Figure 2B,C). Thus, of the six antibodies recognizing VGLUT2, two are specific for VGLUT2 (13H4 and 14E1), four recognize both VGLUT1 and 2 (6D3, 8E11, 9C6, and 12C1), and none recognize VGLUT3. Five of the antibodies bind the luminal face of the transporter, and only one (13H4) binds to the cytoplasmic side.

Since the antibodies were raised against folded, functional VGLUT2,[23] we also determined whether they recognize a linear or structured epitope by Western blotting denatured extract from cells expressing a VGLUT2-EGFP fusion. In contrast to the EGFP antibody, none of the hybridoma antibodies recognize VGLUT2-EGFP by immunoblot (Figure S1). Thus, all of the hybridoma antibodies recognize a folded epitope. The properties of the mAbs are summarized in Table 1.

We previously showed that an Fab fragment of the 8E11 antibody was essential for a high-resolution cryo-EM structure of VGLUT2.[23] The structure of the VGLUT2/8E11 complex showed that 8E11 binds to the lumenal side of VGLUT2, consistent with the staining of unpermeabilized cells in Figure 1B. Specifically, the Fab makes multiple polar contacts with all three short extracellular loops (ECL 4, 5, and 6) in the C-domain of the transporter (Figure 3A). In ECL 4, the backbone carbonyls of V340 and G342 in VGLUT2 hydrogen bond with the backbone amides of L102 and S52 in the 8E11 heavy chain, respectively. Also, in ECL4, the E338 side chain forms a hydrogen bond with Y57 in the 8E11 heavy chain and E344 with the side chains of S52 and S56 in the 8E11 heavy chain (Figure 3A). In ECL5, R409 forms a hydrogen bond with the side chain of Y32 in the 8E11 heavy chain (Figure 3A). In ECL6, the backbone carbonyl of K471 hydrogen bonds with the side chain of S92 in the 8E11 light chain and the side chain of VGLUT2 R473 hydrogen bonds with Y31 and makes a salt bridge with D49 in the 8E11 light chain. Antibody 8E11 thus makes an extensive network of contacts with ECL4–6 of VGLUT2. The sequence of hybridoma antibody 9C6 is almost identical to that of 8E11 (Figure S2), suggesting a very similar interaction with VGLUT2.

To understand how 8E11 recognizes VGLUT1 and 2 but not VGLUT3, we compared the sequence of ECL4–6 from all three isoforms. E344 is the only residue in ECL4–6 conserved in both VGLUT1 and 2 but not VGLUT3, where it is replaced by an alanine (Figure 3B). To determine whether E344 is required for the high-affinity binding of 8E11 to VGLUT2, we replaced this residue with alanine, resulting in a loss of recognition by 8E11 (Figure

3C). Conversely, replacing A348 in VGLUT3 with glutamate was sufficient to confer recognition by 8E11 (Figure 3C). Thus, the residue at this position in ECL4 determines isoform preference by 8E11. The sequence of VGLUT isoforms in ECL4–6 are conserved from rodent to human, predicting that 8E11 and 9C6 hybridomas can also distinguish among the human isoforms (Figure S3).

To determine whether 8E11 interferes with transport, we used an assay for glutamate efflux from HEK293T cells expressing pmVGLUT2. This assay enables the addition of 8E11 to the luminal/extracellular face of VGLUT2 simply by adding 8E11 to the assay buffer. This is not possible with a native preparation such as synaptic vesicles or even after VGLUT reconstitution into proteoliposomes, which exposes the cytoplasmic but not lumenal face of the transporters.[22,25] Cells expressing pmVGLUT2 or EGFP as a control were loaded with [^{3}H]-glutamate (Figure 4A): HEK293T cells accumulate glutamate independent of pmVGLUT2 expression. To mimic uptake by synaptic vesicles, we triggered VGLUT-mediated glutamate efflux by incubating the preloaded cells at low pH (Figure 4A) since lumenal/extracellular protons allosterically activate the VGLUTs.[24] Cells expressing pmVGLUT2 show increased glutamate efflux at pH 5.5 relative to pH 7.4, and control cells show no increase in efflux at low pH (Figure 4B). The addition of 8E11 abolishes the pH-dependent pmVGLUT2-mediated efflux, with no effect of the antibody on efflux from control cells (Figure 4B).

The VGLUTs also exhibit an associated chloride conductance.[24,26–28] This conductance shares many features with glutamate transport including allosteric activation by lumenal/extracellular protons and chloride but is not coupled to glutamate flux and seems to involve a different mechanism although the two anions compete for permeation.[24,27] To determine whether 8E11 influences the VGLUT-associated chloride conductance, we expressed pmVGLUT2 in *Xenopus* oocytes, where a low pH triggers large VGLUT-mediated chloride currents (Figure 5A,B). Incubation of the same oocytes with 8E11 for 10 min effectively eliminated the low pH-activated currents (90.7 ± 1.9% inhibition of low pH-induced current). A parallel experiment with mAb directed to the *C. elegans* VGLUT homologue EAT-4 produced in the same way as 8E11 had no effect on the VGLUT2 chloride conductance (0.2 ± 6.5% inhibition of low pH-induced current), demonstrating the specificity of 8E11 (Figure 5B).

DISCUSSION

In contrast to the extensive and potent pharmacology for plasma membrane neurotransmitter transporters, the vesicular neurotransmitter transporters in general and the VGLUTs in particular lack potent, specific inhibitors. In this study, we characterize a series of monoclonal antibodies to the VGLUTs. Conformation-specific antibodies enable manipulation of their targets for both structural and functional studies, so we raised antibodies against a truncated form of VGLUT2 lacking part of the cytoplasmic N- and C-termini to favor the recognition of nonlinear, structured epitopes. We obtained six new antibodies that recognize structured regions of VGLUT2, including two specific for VGLUT2, four others that also bind to VGLUT1, and none that recognize VGLUT3.

Focusing on the antibody previously used to solve the structure of VGLUT2, we find that 8E11 inhibits both vesicular glutamate transport and the associated chloride conductance. In previous work, we found that glutamate transport and the associated chloride conductance undergo similar allosteric regulation by protons and chloride,[24] and we now find that the similarity between these two activities extends to inhibition by 8E11.

The cryo-EM structure of VGLUT2 provides insight into the mechanism of inhibition by 8E11.[23] The structure shows that 8E11 binds to ECL4–6 of the VGLUT2 C-domain through an extensive network of interactions. The antibody does not bind in the main cavity of the transporter where the substrate is recognized, demonstrating an allosteric mode of inhibition. The requirement for 8E11 on the opposite side of the membrane from the substrate makes it difficult to determine whether this allosteric form of inhibition is noncompetitive. The interactions observed by cryo-EM account for the isoform specificity of 8E11, with binding to VGLUT1 and 2 but not VGLUT3. E344 in ECL4 confers binding specificity toward VGLUT1 and 2, and its replacement by alanine (as in VGLUT3) disrupts the interaction. Conversely, the replacement of alanine by glutamate at this position in VGLUT3 suffices to confer binding by 8E11. Since the site of substrate recognition shows high conservation across VGLUT isoforms, binding to less well-conserved sequences elsewhere in the protein confers specificity not possible with an orthosteric inhibitor. Similar to the development of allosteric modulators for receptors that distinguish among isoforms,[29] it may thus be possible to develop inhibitors that discriminate between other closely related transporters. It would also be of considerable interest to determine how antibodies 13H4 and 14E1 distinguish between VGLUT2 and VGLUT1.

How does antibody binding at an allosteric site within the VGLUT C-domain inhibit transport activity? In general, members of the major facilitator superfamily (MFS) use a rocker-switch mechanism, where N- and C-domains achieve alternating access by a symmetrical rocking movement around the substrate-binding site.[30] Indeed, a comparison of the inwardly and outwardly oriented conformations of the bacterial galactonate transporter DgoT, which is closely related to the VGLUTs, shows only restricted changes within each helical bundle.[31] It might therefore be expected that binding outside the main cavity to a single domain would not perturb the translocation mechanism, but 8E11 appears to trap VGLUT in a lumenal/outward-oriented conformation, which has facilitated structure determination. We propose that, by binding to the three external loops, 8E11 prevents rearrangement within the C-domain required for the transition between conformations. Indeed, structural evidence from other MFS members points to asymmetric transporter intermediates even though inward open and outward open states appear symmetric.[30] Like the nanobodies recently reported,[22] hybridoma 13H4 binds to the cytoplasmic face of VGLUT2, and it would be of interest to determine whether it also inhibits transport and, if so, the mechanism involved.

Recently, multiple studies have used VGLUTs localized at the plasma membrane to study their diverse properties, including glutamate transport,[24] chloride conductance,[23,24,32] and phosphate transport.[33,34] However, the lack of potent, specific, membrane-permeant inhibitors has made it difficult to determine whether the activities monitored reflect the function of VGLUT or an endogenous protein. Our results now show that 8E11 can be

used to inhibit VGLUT in these assays and to confirm that VGLUTs mediate the fluxes monitored.

Supplementary Material

Refer to Web version on PubMed Central for supplementary material.

ACKNOWLEDGMENTS

We thank Dr. David Bulkley, Dr.Zanlin Yu, Mr. Glenn Gilbert, and Mr. Matt Harrington at the UCSF cryo-EM facility and Dr. Corey Hecksel, Dr. Patrick Mitchell, Dr. Lydia-Marie Joubert, and Ms. Lisa Dunn at Stanford-SLAC Cryo-EM Center (S^2C^2) for their support in data acquisition and computation. We thank Dr. Daniel Cawley at VGTI (OHSU) for generating the mAb and advice on working with the antibodies. We also thank Dr. Charles Craik, Dr. Markus Bohn, and Dr.KoliBasu for advice and help in characterizing and working with antibodies.

Funding

This work is supported by R01NS089713 to R.M.S. and R.H.E. and R37MH50712 to R.H.E. F.L. is supported by postdoctoral fellowships from the American Heart Association (17POST33660928) and the National Institute of Mental Health (K99MH119591). The UCSF EM facility is supported by NIH grants S10OD020054 and S10OD021741. Some of this work was performed at the Stanford-SLAC Cryo-EM Center (S2C2), which is supported by the National Institutes of Health Common Fund Transformative High-Resolution Cryo-Electron Microscopy program (U24 GM129541).

REFERENCES

(1). Anne C, and Gasnier B. (2014) Chapter Three - Vesicular Neurotransmitter Transporters: Mechanistic Aspects. Curr. Top. Membr. 73, 149–174. [PubMed: 24745982]

(2). Edwards RH (2007) The Neurotransmitter Cycle and Quantal Size. Neuron 55 (6), 835–858. [PubMed: 17880890]

(3). Maycox PR, Deckwerth T, Hell JW, and Jahn R. (1988) Glutamate Uptake by Brain Synaptic Vesicles. Energy Dependence of Transport and Functional Reconstitution in Proteoliposomes. J. Biol. Chem. 263 (30), 15423–15428. [PubMed: 2902091]

(4). Shioi J, and Ueda T (1990) Artificially imposed electrical potentials drive l-glutamate uptake into synaptic vesicles of bovine cerebral cortex. Biochem. J. 267, 63. [PubMed: 1970243]

(5). Eriksen J, Li F, and Edwards RH (2020) The Mechanism and Regulation of Vesicular Glutamate Transport: Coordination with the Synaptic Vesicle Cycle. Biochim. Biophys. Acta, Biomembr. 1862 (12), 183259.

(6). El Mestikawy S, Wallén-Mackenzie Å, Fortin GM, Descarries L, and Trudeau L-E (2011)From Glutamate Co-Release to Vesicular Synergy: Vesicular Glutamate Transporters. Nat. Rev. Neurosci. 12 (4), 204–216. [PubMed: 21415847]

(7). Fremeau RT, Voglmaier S, Seal RP, and Edwards RH (2004) VGLUTs Define Subsets of Excitatory Neurons and Suggest Novel Roles for Glutamate. Trends Neurosci. 27 (2), 98–103. [PubMed: 15102489]

(8). Fremeau RT, Troyer MD, Pahner I, Nygaard GO, Tran CH, Reimer RJ, Bellocchio EE, Fortin D, Storm-Mathisen J, and Edwards RH (2001)The Expression of Vesicular Glutamate Transporters Defines Two Classes of Excitatory Synapse. Neuron 31 (2), 247–260. [PubMed: 11502256]

(9). Herzog E, Bellenchi GC, Gras C, Bernard V, Ravassard P, Bedet C, Gasnier B, Giros B, and El Mestikawy S. (2001) The Existence of a Second Vesicular Glutamate Transporter Specifies Subpopulations of Glutamatergic Neurons. J. Neurosci. 21 (22), RC181–RC181.

(10). Fremeau RT, Burman J, Qureshi T, Tran CH, Proctor J, Johnson J, Zhang H, Sulzer D, Copenhagen DR, Storm-Mathisen J, Reimer RJ, Chaudhry FA, and Edwards RH (2002) The Identification of Vesicular Glutamate Transporter 3 Suggests Novel Modes of Signaling by Glutamate. Proc. Natl. Acad. Sci. U. S. A. 99 (22), 14488–14493.

(11). Gras C, Herzog E, Bellenchi GC, Bernard V, Ravassard P, Pohl M, Gasnier B, Giros B, and El Mestikawy S. (2002) A Third Vesicular Glutamate Transporter Expressed by Cholinergic and Serotoninergic Neurons. J. Neurosci. 22 (13), 5442–5451. [PubMed: 12097496]

(12). Seal RP, Akil O, Yi E, Weber CM, Grant L, Yoo J, Clause A, Kandler K, Noebels JL, Glowatzki E, Lustig LR, and Edwards RH (2008) Sensorineural Deafness and Seizures in Mice Lacking Vesicular Glutamate Transporter 3. Neuron 57 (2), 263–275. [PubMed: 18215623]

(13). Moechars D, Weston MC, Leo S, Callaerts-Vegh Z, Goris I, Daneels G, Buist A, Cik M, van der Spek P, Kass S, Meert T, D'Hooge R, Rosenmund C, and Hampson RM (2006) Vesicular Glutamate Transporter VGLUT2 Expression Levels Control Quantal Size and Neuropathic Pain. J. Neurosci. 26 (46), 12055–12066.

(14). Wallen-Mackenzie A, Gezelius H, Thoby-Brisson M, Nygard A, Enjin A, Fujiyama F, Fortin G, and Kullander K. (2006) Vesicular Glutamate Transporter 2 Is Required for Central Respiratory Rhythm Generation But Not for Locomotor Central Pattern Generation. J. Neurosci. 26 (47), 12294–12307.

(15). Wojcik SM, Rhee JS, Herzog E, Sigler A, Jahn R, Takamori S, Brose N, and Rosenmund C. (2004) An Essential Role for Vesicular Glutamate Transporter 1 (VGLUT1) in Postnatal Development and Control of Quantal Size. Proc. Natl. Acad. Sci. U. S. A. 101 (18), 7158–7163. [PubMed: 15103023]

(16). Moriyama Y, and Yamamoto A. (1995) Vesicular L-Glutamate Transporter in Microvesicles from Bovine Pineal Glands. Driving Force, Mechanism of Chloride Anion Activation, and Substrate Specificity. J. Biol. Chem. 270 (38), 22314–22320.

(17). Winter HC, and Ueda T. (1993) Glutamate Uptake System in the Presynaptic Vesicle: Glutamic Acid Analogs as Inhibitors and Alternate Substrates. Neurochem. Res. 18 (1), 79–85. [PubMed: 8096630]

(18). Roseth S, Fykse EM, and Fonnum F. (1995) Uptake of L-Glutamate into Rat Brain Synaptic Vesicles: Effect of Inhibitors That Bind Specifically to the Glutamate Transporter. J. Neurochem. 65 (1), 96–103. [PubMed: 7790899]

(19). Tamura Y, Ogita K, and Ueda T. (2014) A New VGLUT-Specific Potent Inhibitor: Pharmacophore of Brilliant Yellow. Neurochem. Res. 39 (1), 117–128. [PubMed: 24248859]

(20). Cao Q, Zhao K, Zhong XZ, Zou Y, Yu H, Huang P, Xu T-L, and Dong X-P (2014) SLC17A9 Protein Functions asa Lysosomal ATP Transporter and Regulates Cell Viability. J. Biol. Chem. 289 (33), 23189–23199.

(21). Pietrancosta N, Djibo M, Daumas S, El Mestikawy S, and Erickson JD (2020) Molecular, Structural, Functional, and Pharmacological Sites for Vesicular Glutamate Transporter Regulation. Mol. Neurobiol. 57 (7), 3118–3142. [PubMed: 32474835]

(22). Schenck S, Kunz L, Sahlender D, Pardon E, Geertsma ER, Savtchouk I, Suzuki T, Neldner Y, Štefanić S, Steyaert J, Volterra A., and Dutzler R. (2017) Generation and Characterization of Anti-VGLUT Nanobodies Acting as Inhibitors of Transport. Biochemistry 56 (30), 3962–3971. [PubMed: 28731329]

(23). Li F, Eriksen J, Finer-Moore J, Chang R, Nguyen P, Bowen A, Myasnikov A, Yu Z, Bulkley D, Cheng Y, Edwards RH, and Stroud RM (2020) Ion Transport and Regulation in a Synaptic Vesicle Glutamate Transporter. Science 368 (6493), 893–897.. [PubMed: 32439795]

(24). Eriksen J, Chang R, McGregor M, Silm K, Suzuki T, and Edwards RH (2016) Protons Regulate Vesicular Glutamate Transporters through an Allosteric Mechanism. Neuron 90 (4), 768–780. [PubMed: 27133463]

(25). Preobraschenski J, Zander JF, Suzuki T, Ahnert-Hilger G, and Jahn R. (2014)Vesicular Glutamate Transporters Use Flexible Anion and Cation Binding Sites for Efficient Accumulation of Neurotransmitter. Neuron 84 (6), 1287–1301. [PubMed: 25433636]

(26). Bellocchio EE, Reimer RJ, Fremeau RT, and Edwards RH (2000) Uptake of Glutamate into Synaptic Vesicles by an Inorganic Phosphate Transporter. Science 289 (5481), 957–960. [PubMed: 10938000]

(27). Chang R, Eriksen J, and Edwards RH (2018) The Dual Role of Chloride in Synaptic Vesicle Glutamate Transport. eLife 7, e34896.

(28). Schenck S, Wojcik SM, Brose N, and Takamori S. (2009) A Chloride Conductance in VGLUT1 Underlies Maximal Glutamate Loading into Synaptic Vesicles. Nat. Neurosci. 12 (2), 156–162. [PubMed: 19169251]

(29). Foster DJ, and Conn PJ (2017) Allosteric Modulation of GPCRs: New Insights and Potential Utility for Treatment of Schizophrenia and Other CNS Disorders. Neuron 94 (3), 431–446. [PubMed: 28472649]

(30). Drew D, North RA, Nagarathinam K, and Tanabe M. (2021) Structures and General Transport Mechanisms by the Major Facilitator Superfamily (MFS). Chem. Rev. 121 (9), 5289–5335. [PubMed: 33886296]

(31). Leano JB, Batarni S, Eriksen J, Juge N, Pak JE, Kimura-Someya T, Robles-Colmenares Y, Moriyama Y, Stroud RM, and Edwards RH (2019) Structures Suggest a Mechanism for Energy Coupling by a Family of Organic Anion Transporters. PLoS Biol. 17 (5), e3000260.

(32). Martineau M, Guzman RE, Fahlke C, and Klingauf J. (2017) VGLUT1 Functions as a Glutamate/Proton Exchanger with Chloride Channel Activity in Hippocampal Glutamatergic Synapses. Nat. Commun. 8 (1), 2279. [PubMed: 29273736]

(33). Cheret C, Ganzella M, Preobraschenski J, Jahn R, and Ahnert-Hilger G. (2021) Vesicular Glutamate Transporters (SLCA17 A6, 7, 8) Control Synaptic Phosphate Levels.Cell Rep. 34 (2), 108623.

(34). Preobraschenski J, Cheret C, Ganzella M, Zander JF, Richter K, Schenck S, Jahn R, and Ahnert-Hilger G. (2018) Dual and Direction-Selective Mechanisms of Phosphate Transport by the Vesicular Glutamate Transporter.Cell Rep. 23 (2), 535–545. [PubMed: 29642010]

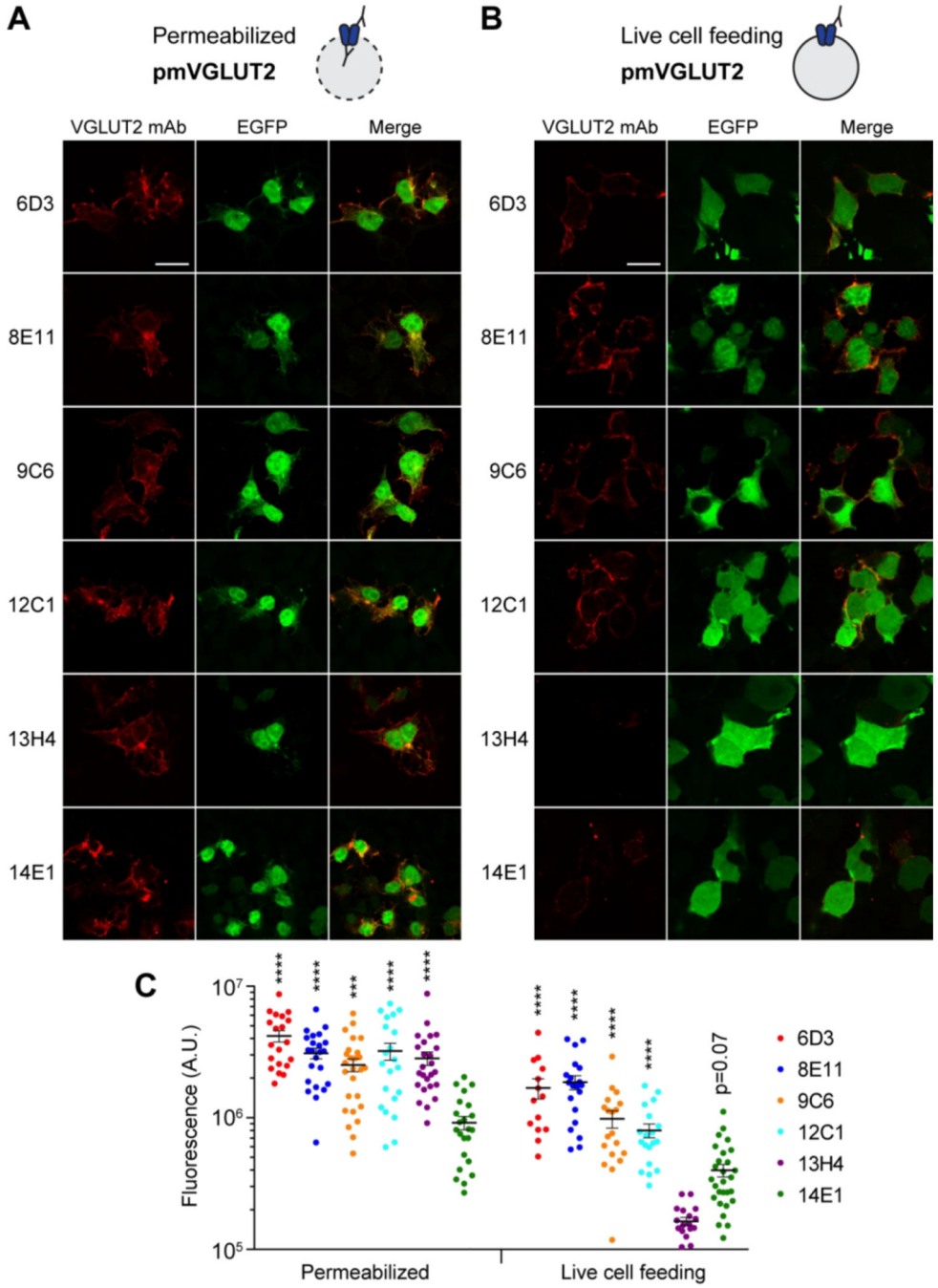

Figure 1.

Novel monoclonal antibodies bind VGLUT2 from different sides of the membrane. HEK293T cells coexpressing pmVGLUT2 and EGFP were stained with VGLUT2 mAb hybridoma supernatants. (A) After fixation and permeabilization, all VGLUT2 mAbs label only transfected cells identified with EGFP. (B) Live HEK293T cells were incubated with hybridoma supernatants. 6D3, 8E11, 9C6, 12C1, and 14E1 but not 13H4 bind to intact cells expressing pmVGLUT2. 13H4 thus binds to the cytoplasmic face of VGLUT2. Scale bar, 20 μm. (C) Quantification of total VGLUT2 mAb fluorescence from EGFP+ cells for each

of the conditions in parts A and B. $n = 14–26$ cells for each condition. Left panel: ***, $p < 0.001$; ****, $p < 0.0001$ compared to 14E1 by Kruskal–Wallis. Right panel: ****, $p < 0.0001$ relative to 13H4 by Kruskal–Wallis.

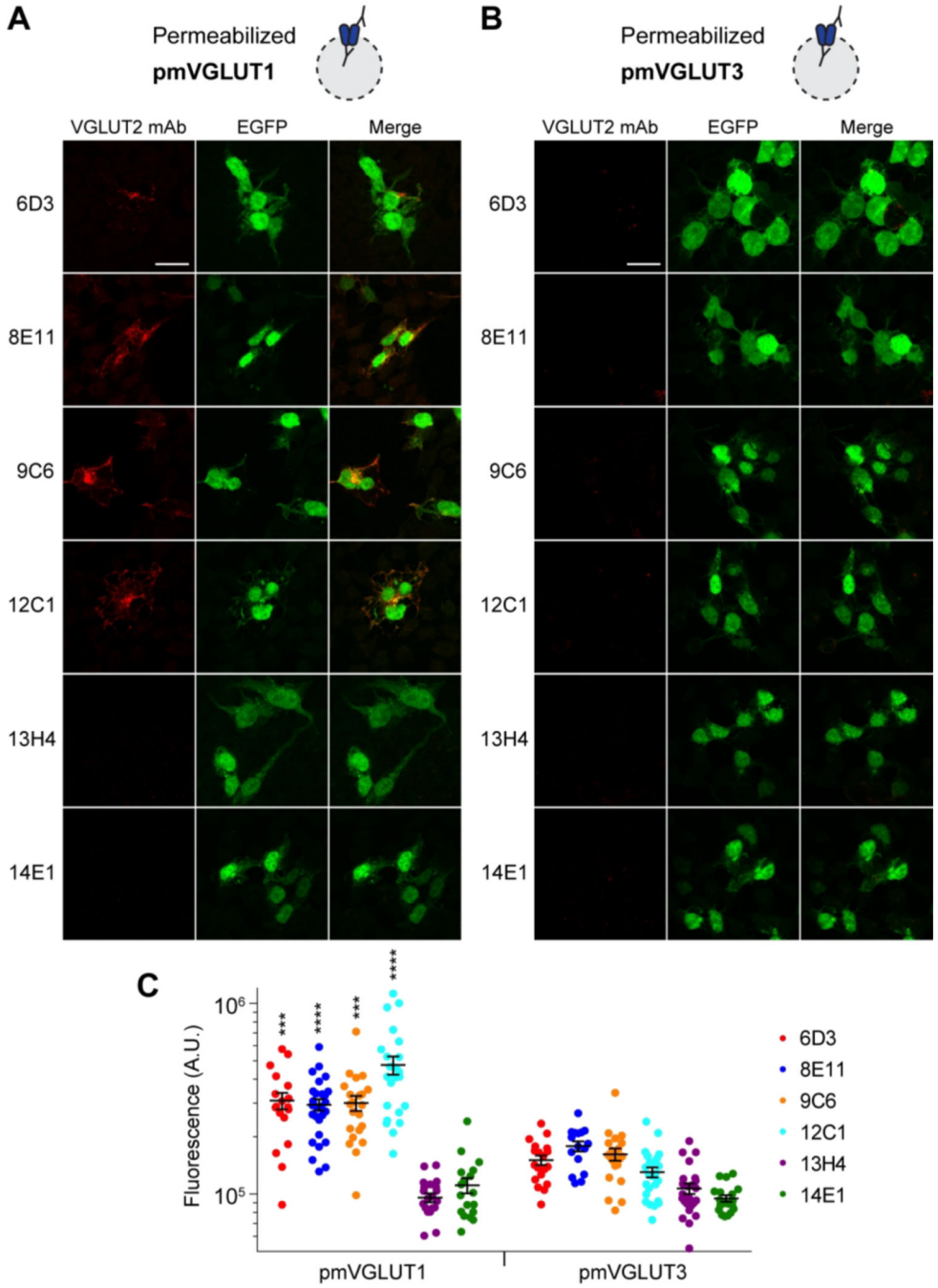

Figure 2.

VGLUT isoform specificity of novel VGLUT2 mAbs. Fixed, permeabilized HEK293T cells expressing pmVGLUT1 (A) or pmVGLUT3 (B) were incubated with VGLUT2 mAb hybridoma supernatants as in Figure 1A. (A) mAbs 6D3, 8E11, 9C6, and 12C1 bind to cells expressing pmVGLUT1, whereas 13H4 and 14E1 do not. (B) None of the mAbs bind to cells expressing pmVGLUT3. Scale bar = 20 μm. (C) Quantification of total VGLUT2 mAb fluorescence from EGFP+ cells for each of the conditions in panels A and B. n = 16–25 cells

for each condition. ***, $p < 0.001$; ****, $p < 0.0001$ compared to either 13H4 or 14E1 by Kruskal–Wallis.

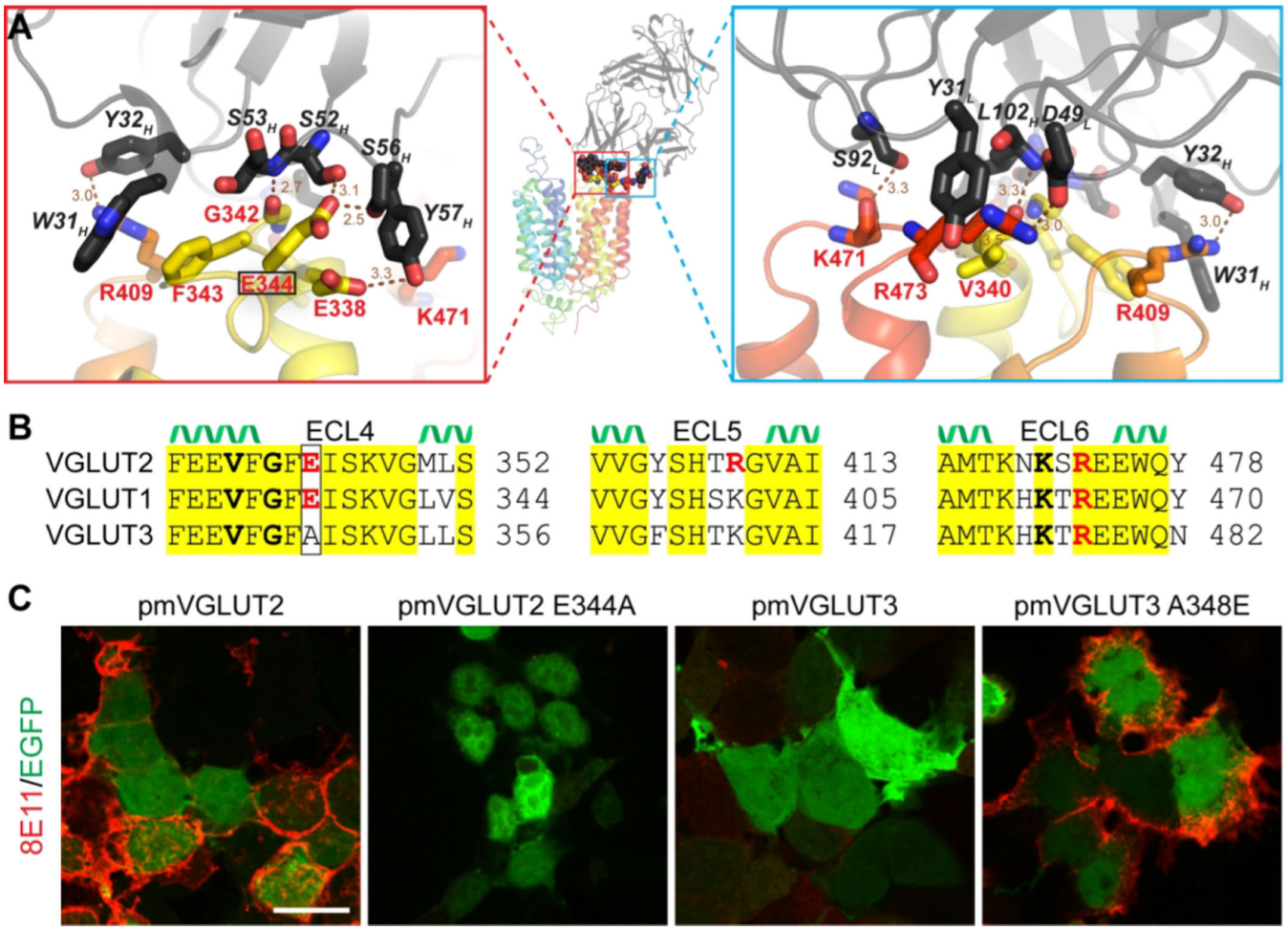

Figure 3.

Structure of VGLUT2–8E11 reveals the basis of isoform specificity. (A) Cryo-EM structure of rat VGLUT2 (rainbow) and Fab 8E11 (black) with the interface enlarged on the left and right (PDB: 6V4D). The sequence on the right is rotated 180° around an axis perpendicular to the membrane. (B) Alignment of ECL4–6 of VGLUT1–3 with conserved residues highlighted in yellow. VGLUT residues contacting 8E11 are indicated in bold and side-chain interactions in red. Glutamate 344 (boxed) is the only residue conserved in VGLUT1 and 2 but not VGLUT3. (C) Live cell feeding for pmVGLUT2, pmVGLUT2 E344A, pmVGLUT3, and pmVGLUT3 A348E confirms the requirement of 8E11 for the divergent ECL4 glutamate. Scale bar = 20 μm.

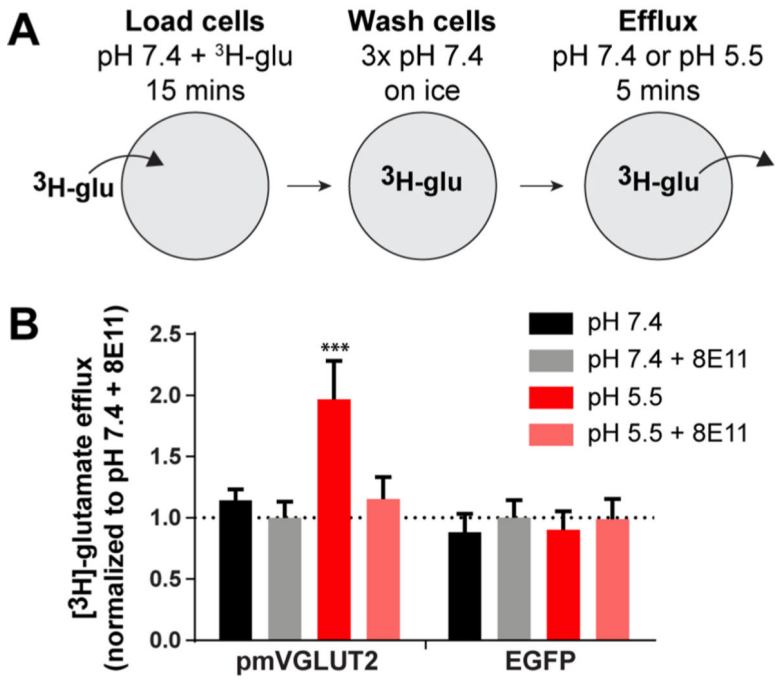

Figure 4.

8E11 inhibits glutamate transport by VGLUT2. (A) Assay for glutamate efflux. HEK293T cells are loaded with ^{3}H-glutamate in the absence or presence of 8E11 and washed in cold Ringer's solution before incubation in efflux buffer at either pH 7.4 or pH 5.5. (B) Efflux of ^{3}H-glutamate from HEK293T cells expressing pmVGLUT2 + EGFP or EGFP alone. Efflux was measured with or without 8E11 at pH 7.4 and pH 5.5 ($n = 5$). Data indicate the mean ± SEM *** $p < 0.001$ compared to all other conditions, by two-way ANOVA.

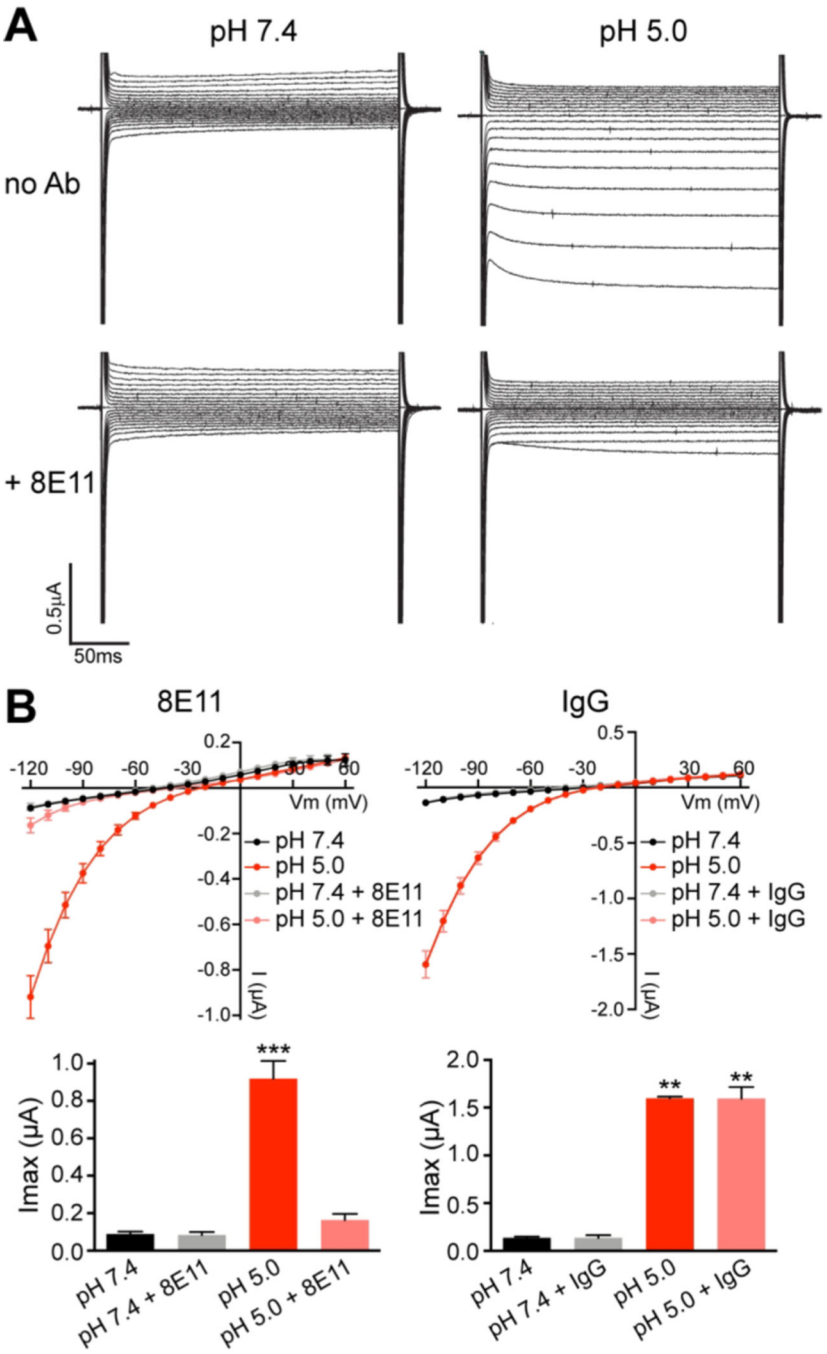

Figure 5.

8E11 inhibits the chloride conductance associated with VGLUT2. (A) Representative traces of the currents from an oocyte expressing pmVGLUT2-HA, at either pH 7.4 or 5.0, without or with 8E11. (B) *I–V* curves of the currents from *X. laevis* oocytes expressing pmVGLUT2-HA (top) and bar graphs of the same currents at −120 mV (bottom). The currents were recorded at pH 7.4 and pH 5.5 before and after incubation with mAb 8E11 or an EAT-4 (IgG) antibody as a negative control. $n = 7$ oocytes for 8E11, $n = 3$ oocytes for EAT-4 mAb. Data indicate the mean ± SEM. Bottom, ***, $p < 0.001$ by two-way ANOVA

compared to all other conditions (left) and **, $p < 0.01$ by two-way ANOVA compared to both pH 7.4 conditions (right).

Table 1.

Properties of the VGLUT2 mAbs

mAb	binding	3D epitope	VGLUT1	VGLUT2	VGLUT3
6D3	lumenal	yes	+	+	-
8E11	lumenal	yes	+	+	-
9C6	lumenal	yes	+	+	-
12C1	lumenal	yes	+	+	-
13H4	cytosolic	yes	-	+	-
14E1	lumenal	yes	-	+	-